COMMUNICATION

Exploring through-bond and through-space magnetic communication in 1,3,2-dithiazolyl radical complexes

Received 00th January 20xx,
Accepted 00th January 20xx

DOI: 10.1039/x0xx00000x

Dominique Leckie,[a] Nadia Stephaniuk,[a] Ana Arauzo,[b] Javier Campo[b] and Jeremy M. Rawson.[a]*

Reaction of the methyl-benzodithiazolyl radical (MBDTA) with $M(hfac)_2$ complexes (M = Mn, Co, Zn) affords the complexes $M(hfac)_2(MBDTA)_2$. Strong antiferromagnetic exchange interactions are observed between M(II) ions and the two S = ½ radicals (M = Mn, Co), whereas weak antiferromagnetic interactions are observed between radicals when using the diamagnetic Zn(II) ion. Strong intermolecular exchange coupling is also evident in $Mn(hfac)_2(MBDTA)_2$ and attributed to π^*–π^* contacts between MBDTA radicals which are absent for the Co and Zn derivatives.

Significant efforts have been made to use the so-called "metal-radical approach" to molecular magnetism in recent years in which exchange coupling between a metal and a paramagnetic ligand is proposed to facilitate more effective magnetic communication between metal ions than occurs via conventional diamagnetic ligands.[1] In addition, recent work has focused on using spin-carrying ligands to enhance the total spin ground state of metal complexes[1] and has been proposed to suppress quantum tunnelling in single molecule magnets.[1] In addition, studies of metal-radical interactions can provide insight into a range of metallo-enzymes in which non-innocent redox-active ligands are proposed to play an important role in their biological function.[2] To this end, the development of new families of paramagnetic ligands for metal coordination are highly desirable and a range of stable heterocyclic ligands have emerged including nitronyl nitroxide (NIT),[3] verdazyl (vd),[4] dithiadiazolyl (DTDA),[5] benzotriazinyl (btz),[6] triarylmethyl (pyBTM),[7] thiatriazinyl (TTA)[8] and tetrazinyl ($tz^{\bullet-}$) radicals[9] *inter alia* (Scheme 1). The family of 1,3,2-dithiazolyl (DTA) radicals have previously been examined as building blocks for the construction of organic 'spin transition' materials, with a number of derivatives exhibiting solid state phase transitions between S = 0 'pancake dimers' and two S = ½ monomers.[10] Selected salts of the benzobis(1,3,2-dithiazolyl) radical cation $BBDTA^{+\bullet}$ (Scheme 2) have shown magnetic order[11] and the parent benzo-1,3,2-dithiazolyl exhibits an unusual "double-melting" from a π*–π* dimer[12] to a structurally unknown paramagnetic phase which exhibits magnetic ordering at 11 K.[13] The coordination chemistry of DTA radicals is less well developed. A number of N-donor DTA adducts to diamagnetic *p*-block Lewis acids have been reported[14] and a single coordination complex to a paramagnetic metal ion $Cu(hfac)_2(TTTA)$ (TTTA, see Scheme 2) has been described.[15] In many cases radicals can be rather poor Lewis bases and incorporation of the radical into a polydentate ligand framework is desirable to assist metal coordination[1] and/or a

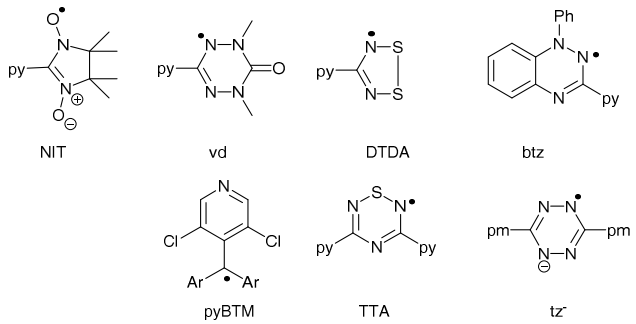

Scheme 1. Selected coordinating radical ligands

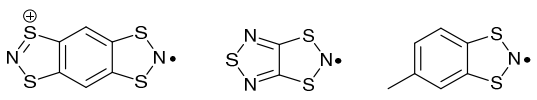

Scheme 2. Selected 1,3,2-dithiazolyl (DTA) radicals

[a] *Dept of Chemistry & Biochemistry, The University of Windsor, 401 Sunset Ave, Windsor, ON, Canada, N9B 3P4. E-mail jmrawson@uwindsor.ca*
[b] *Departamento de Física de la Materia Condensada, Facultad de Ciencias, and Instituto de Ciencia de Materiales de Aragon, CSIC-Universidad de Zaragoza, E-50009 Zaragoza, Spain.*

† Footnotes relating to the title and/or authors should appear here.
Electronic Supplementary Information (ESI) available: structural information in cif format (CCDC deposition numbers 1913687 (**1**), 1914612 (**2**) and 1913688 (**3**), synthetic details for the formation and characterization of **1** – **3**; SC-XRD, PXRD, IR and EPR studies on **1** – **3**; computational studies on the intermolecular exchange via S···S and π···π interactions. See DOI: 10.1039/x0xx00000x

strongly Lewis acidic metal ion such as $M(hfac)_2$ (hfac = hexafluoroacetylacetonate anion) have been implemented.[16] In the current paper we describe the coordination chemistry of the monodentate methylbenzo- 1,3,2-dithiazolyl radical (MBDTA, Scheme 2).[17] In this family of radicals substantial spin density (*ca.* 50%) is located on the heterocyclic N-donor atom[18] which should favour strong metal-ligand magnetic communication. MBDTA was prepared according to the literature method[17] and reacted with $M(hfac)_2$ (M = Mn, Co, Zn) in a 1.95:1 stoichiometry in CH_2Cl_2 at room temperature (see ESI-1). After 30 minutes the solvent was evaporated and the dark residue sublimed *in vacuo* (10^{-1} torr) to afford single crystals of $M(hfac)_2(MBDTA)_2$ suitable for X-ray diffraction. PXRD studies on $Mn(hfac)_2(MBDTA)_2$ both after removal of solvent and after sublimation clearly reveal complex formation occurs prior to sublimation (Figure S1).

The structures of the Co(II) complex $Co(hfac)_2(MBDTA)_2$ (**1**) and Zn(II) complex $Zn(hfac)_2(MBDTA)_2$ (**2**) are isomorphous, crystallizing in the triclinic space group P-1 with half a molecule in the asymmetric unit (Figure 1). For **1** and **2** the M-N bond lengths are 2.086(4) and 2.180(3) Å respectively. The Co-O bond lengths in **1** are 2.042(3) – 2.060(3) Å, whereas for **2** the Zn-O bond lengths are 2.039(2) – 2.066(2) Å. The bond lengths to Co are consistent with high spin Co(II) expected for an N_2O_4 donor set. The MBDTA ring plane in **1** and **2** lies between the two $hfac^-$ anions (Figure S5).

The structure of $Mn(hfac)_2(MBDTA)_2$ (**3**) is shown in Figure 2 and, in contrast to **1** and **2**, adopts the higher symmetry trigonal R-3 space group, with half a molecule in the asymmetric unit. The structure comprises a 6-coordinate Mn(II) centre with two chelate $hfac^-$ ligands in the equatorial plane and two axial MBDTA ligands. The Mn-N bond length is 2.205(4) Å, whereas the Mn-O bond lengths are 2.090(8) and 2.154(7) Å respectively. Structurally the conformation of **3** is different from **1** and **2**. In all three structures the four CF_3 groups can be considered to generate two clefts; one which dissects the two $hfac^-$ ligands and one which is oriented between the $hfac^-$ ligands. In **1** and **2** the plane of the MBDTA radical is located within the 'cleft' between the $hfac^-$ ligands, whereas in the case of **3** the MBDTA adopts an alternative geometry which dissects both $hfac^-$ ligands (Figure 3). The Mn-O and Mn-N bond lengths in **3** are longer than in **1** and **2** and it appears that with less steric crowding the MBDTA ring adopts an orientation which dissects

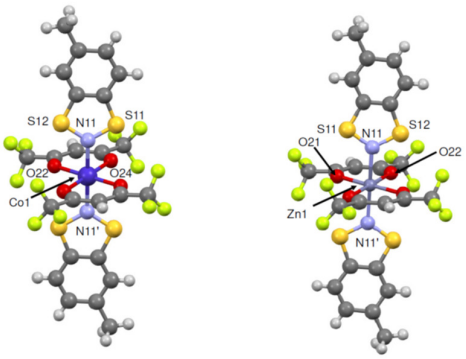

Figure 1. Crystal structure of $Co(hfac)_2(MBDTA)_2$ (**1**) (left) and $Zn(hfac)_2(MBDTA)_2$ (**2**) (right)

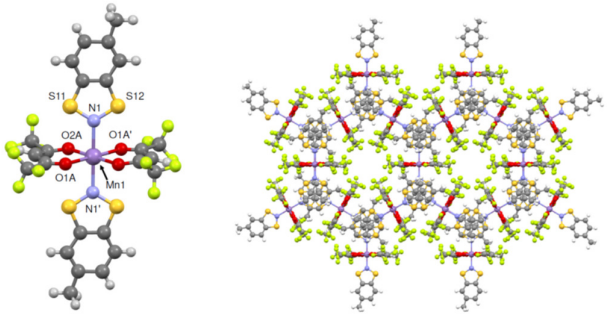

Figure 2. (left) crystal structure of $Mn(hfac)_2(MBDTA)_2$ (1); (right) packing of 1 viewed down the crystallographic c-axis highlighting the hexagonal packing motif.

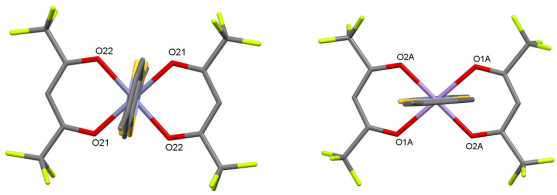

Figure 3. (left) crystal structure of (left) $Co(hfac)_2(MBDTA)_2$ (**2**) and (right) $Mn(hfac)_2(MBDTA)_2$ (**3**) (right), highlighting the orientation of the MBDTA radical with respect to the $M(hfac)_2$ plane.

the $hfac^-$ ligands, whereas the compressed M-N and M-O bond lengths in **1** and **2** appear to favour the cleft in which the MBDTA is located between $hfac^-$ ligands. PXRD studies on **1**, **2** and **3** (see Figure S2) reveal no evidence for either species adopting the alternative packing motif. The packing of **3** generates a hexagonal packing motif (Figure 2) with channels of ca. 7.4 Å diameter with a hydrophobic interior made up of CF_3 groups. Taking into account the van der Waals radius of F (1.47 Å), these channels are very narrow and there was no evidence from the crystal structure for inclusion of gas or solvent molecules within the pores.

Variable temperature magnetic measurements on **1** reveal a rapid decrease in χT from 2.36 emu·K·mol^{-1} at room temperature down to 0.70 emu·K·mol^{-1} around 70 K where χT forms a plateau (Figure 4). The value of χT decreases again below 10 K to a value of 0.27 emu·K·mol^{-1} at 2 K. The general decrease in the high temperature regime is consistent with strong antiferromagnetic coupling between the two S = ½ radicals and the octahedral Co(II) ion which has a ^4T term, leading to an S_T = ½ spin ground state. In the low temperature regime (T < 50 K) the data follow Curie-Weiss behaviour with C = 0.707 emu·K·mol^{-1} (consistent with S_T = ½ and g = 2.74) and a Weiss constant θ = -2.9 K. The large g value for complex **1** originates from the presence of unquenched orbital angular momentum derived from the Co(II) ion. Modelling the temperature dependence of **1** in the high temperature region is complicated by the significant single ion anisotropy associated with the Co(II) ion as well as substantial exchange coupling. Nevertheless, the decrease in χT and subsequent plateau observed for **1** in the high temperature region is comparable with that reported by Murray and co-workers for an octahedral Co(II) complex bearing two S = ½ radicals.[19] In the low temperature region, the S_T = ½ ground state can exhibit no zero

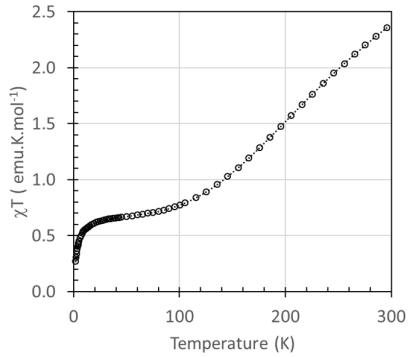

Figure 4. Temperature dependence of χT for **1**. The dotted line is a guide for the eye

field splitting and the Weiss constant (-2.9 K) reflects weak intermolecular antiferromagnetic interactions. In order to probe the nature of radical···radical exchange within these complexes, we examined the magnetism of **2** in which the d^{10} Zn(II) ion is diamagnetic. Complex **2** obeys Curie-Weiss behaviour down to 30 K with C = 0.754 emu·K·mol^{-1} and θ = -19 K, consistent with antiferromagnetic exchange between S = ½ ions (C = 0.750 emu·K·mol^{-1} for g = 2.0). A plot of χ vs T reveals a maximum in χ around 9.0 K (Figure 4) and a one parameter fit to the Bleaney-Bowers expression[20] for two interacting S = ½ spins ($\hat{H}$ = -2$J\hat{S}_1\hat{S}_2$) afforded J/k = -4.7(1) K (g fixed at 2.005). A small increase in χ in the low temperature region (T < 5 K) was assigned to a small number of S = ½ defects in the lattice.

For complex **3**, a plot of χT *vs* T (Figure 5) reveals a room temperature moment of 3.16 emu·K·mol^{-1}, considerably lower than that expected for two non-interacting S = ½ and one S = $^5/_2$ spins (5.125 emu·K·mol^{-1}). Strong intramolecular antiferromagnetic exchange interactions between S = $^5/_2$ Mn(II) and two S = ½ radicals would be expected to give rise to a plateau for an S_T = $^3/_2$ ground state around C = 1.875 emu·K·mol^{-1} (g = 2.0) but χT decreases steadily upon cooling to 0.114 emu·K·mol^{-1} at 2 K. In the absence of significant single ion anisotropy, the unexpected and continued decrease in χT reflects the presence of additional, strong, intermolecular antiferromagnetic interactions. An initial fit of the magnetic

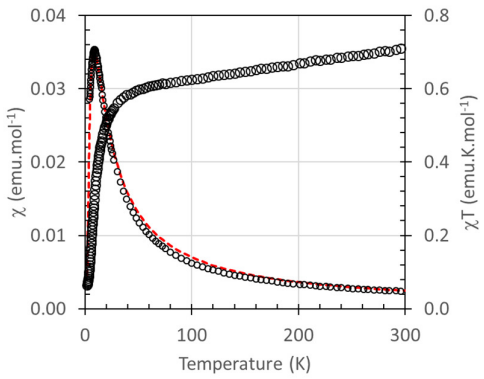

Figure 5. Temperature dependence of χ and χT for **2** with the dotted red line reflecting the fit to the maximum in χ *vs* T Bleaney-Bowers expression for two interacting S = ½ species [g = 2.007 (fixed), J= -4.7(1) cm^{-1}].

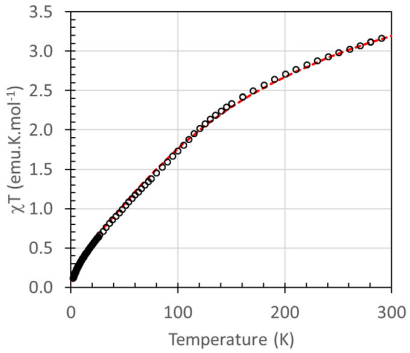

Figure 6. (top) Temperature dependence of χ^{-1} for **3** with the dotted line reflecting the fit to Curie-Weiss behaviour in the high temperature region; (bottom) temperature dependence of χT for **3** with the dotted line reflecting the best two-parameter fit to the data (see text).

data using the simple isotropic exchange Hamiltonian $\hat{H}$ = -2$J[\hat{S}_1\hat{S}_2 + \hat{S}_1\hat{S}_3]$ (using fixed g values for Mn(II) and DTA radicals of 1.98 and 2.006, typical for these systems) proved inadequate, predicting a plateau around χT = 1.875 emu·K·mol^{-1}) consistent with an S_T = 3/2 ground state. Including an additional exchange term for intramolecular radical···radical interactions did not improve the fit since this term is (a) likely small based on the weak nature of radical···radical exchange in **2** and (b) only enhances or suppresses the rate at which full population of the S_T = 3/2 state is achieved and does not reflect the observed decrease in χT below that expected for an S_T = 3/2 ground state. In the absence of significant spin anisotropy, the decrease in χT suggested the presence of substantial intermolecular exchange. The inclusion of an additional mean field term (zJ') within PHI[21] provided a very good fit to the data across the entire temperature range with J/k = -25.3(6) K and zJ'/k = -9.1(1) K. However, the similar magnitudes of the intra- and inter-molecular exchange coupling suggest that consideration of the magnetism of **3** as a simple isolated three-spin model is inappropriate. In the limit where J' >> J then antiferromagnetic coupling between radicals would quench the ligand paramagnetism leading to weakly exchange coupled S = 5/2 spins in the low temperature regime which is not reflected in the observed χT data confirming the comparable nature of intra- and inter-molecular exchange.

The weak nature of the intermolecular interactions in both **1** and **2** are in stark contrast to **3** and likely arises from the different packing in isomorphous **1** and **2** (triclinic P-1) in relation to **3** (trigonal R-3). Previous work by Preuss has shown intermolecular exchange coupling between clusters *via* S···O contacts between DTDA radicals (where the S atom bears substantial spin density) and $hfac^-$ ligands (which bear a little spin density) become important at low temperature.[22] In the current series of complexes, both **1** and **2** exhibit close 'edge-to-edge' S···S contacts (3.558(1) Å for **2**) which are close to the BDTA molecular plane (Figure S6), leading to rather poor orbital overlap and may be expected to lead to modest exchange coupling. Conversely in **3,** the intermolecular S···S contacts comprise an out-of-plane π–π type contact at 3.611(4) Å (Figure S6), reflected in a much larger intermolecular exchange coupling interaction associated with efficient SOMO-SOMO

interactions. Computational studies on these intermolecular exchange couplings (ESI-6) confirm this perspective with near-zero computed exchange coupling (J_{inter} = −1 cm^{-1}) for the in-plane contacts present in **1** and **2,** but strong antiferromagnetic coupling associated with the π···π contact (J_{inter} = −360 cm^{-1}) in **3**.

In summary, we have shown that MBDTA acts as a monodentate donor to Lewis acidic $M(hfac)_2$ complexes, providing efficient magnetic exchange between π-based radicals and metal *d*-based electrons. The manifestation of substantial intermolecular exchange coupling in **3** augers well for the construction of future materials in which the propagation of efficient, through-space magnetic exchange interactions may lead to bulk magnetic order.

Conflicts of interest

There are no conflicts to declare.

Notes and references

‡ J.M.R. would like to thank NSERC for financial support. A.A. and J.C. acknowledge support from grant MAT2015-68200-C2–2-P from the Ministerio de Economía y Competividad of Spain and the European Regional Development Fund. Additional support from Diputacioń General de Aragoń (DGA-M4) is also acknowledged.

ORC-ID A. Arauzo 0000-0002-5999-341X; J.M. Rawson 0000-0003-0480-5386; N. Stephaniuk 0000-0002-0749-5355; D. Leckie 0000-0002-5348-6046; J. Campo 0000-0002-3600-1721

1 (a) A. Caneschi, D. Gatteschi, R. Sessoli and P. Rey, *Accts. Chem. Res.*, 1989, **22**, 392 – 398; (b) S. Demir, I-R. Jeon, J. R. Long and T. D. Harris, *Coord. Chem. Rev.*, 2015, **289 – 290**, 149 – 176.

2 W. Kaim and B. Schwederski, *Coord. Chem. Rev.*, 2010, **254**, 1580 – 1588.

3 (a) X. Meng, W. Shi and P. Cheng, *Coord. Chem. Rev.*, 2019 **378**, 134 – 150; (b) J. Sun, Z. Sun, L. Li and J.-P. Sutter, *Inorg. Chem.*, 2018, **57**, 7507 – 7511; (c) H. Li, J. Sun, M. Yang, Z. Sun, J. Tang, Y. Ma, L. Li, *Inorg. Chem.* 2018, **57**, 9757 – 9765; (d) J. Wang, J.-N. Li, S.-L. Zhang, X.-H. Zhao, D. Shao and X.-Y. Wang, *Chem. Commun.*, 2016, **52**, 5033 – 5036.

4 (a) B. D. Koivisto and R. G. Hicks, *Coord. Chem. Rev.*, 2005, **249**, 2612 – 2630; (b) C. A. Sanz, Z. R. McKay, S. W. MacLean, B. O. Patrick and R. G. Hicks, *Dalton Trans.*, 2017, **46**, 12636 – 12644; (c) G. Novitchi, S. Shova, Y. Lan, W. Wernsdorfer and C. Train, *Inorg. Chem.*, 2016, **55**, 12122 – 12125; (d) A. B. Solea, T. Wohlhauser, P. Abbasi, Y. Mongbanziama, A. Crochet, K. M. Fromm, G. Novitchi, C. Train, M. Pilkington, O. Mamula, *Dalton Trans*. 2018, **47**, 4785 – 4789.

5 (a) K. E. Preuss, *Coord. Chem. Rev.*, 2015, **289 – 290**, 49 – 61; (b) D. A. Haynes, L. J. van Laeren and O. Q. Munro, *J. Amer. Chem. Soc.* 2017, **139**, 14620 – 14637; (c) E. M. Fatila, R. Clérac, M. Rouzières, D. V. Soldatov, M. Jennings and K. E. Preuss, *J. Amer. Chem. Soc.*, 2013, **135**, 13298 – 13301; (d) C. A. Michalowicz, M. B. Mills, E. Song, D. V. Soldatov, P. D. Boyle, M. Rouzières, R. Clérac and K. E. Preuss, *Dalton Trans.*, 2019, **48**, 4514 – 4519.

6 (a) I. S. Morgan, A. Mansikkamäki, G. A. Zissimou, P. A. Koutentis, M. Rouzières, R. Clérac and H. M. Tuononen, *Chem. – Eur. J.*, 2015, **21**, 15843 – 15853; (b) I. S. Morgan, A. Mansikkamäki, M. Rouzières, R. Clérac and H. M. Tuononen, *Dalton Trans.*, 2017, **46**, 12790 – 12793; (c) I. S. Morgan, A. Peuronen, M. M. Hänninen, R. W. Reed, R. Clérac and H. M. Tuononen, *Inorg. Chem.*, 2013, **53**, 33 – 35.

7 (a) A. Abdurahman, Q. Peng, O. Ablikim, X. Ai and F. Li, *Materials Horizons* 2019, DOI: 10.1039/C9MH00077A. (b) Y. Hattori, S. Kimura, T. Kusamoto, H. Maeda, H. Nishihara, *Chem. Commun.*, 2018, **54**, 615 – 618; (c) Y. Hattori, T. Kusamoto, T. Sato and H. Nishihara, *Chem. Commun.*, 2016, **52**, 13393 – 13396.

8 K. L. Harriman, I. A. Kühne, A. A. Leitch, I. Korobkov, R. Clérac, M. Murugesu and J. L. Brusso, *Inorg. Chem.*, 2016, **55**, 5375 – 5383; (b) K. L. Harriman, A. A. Leitch, S. A. Stoian, F. Habib, J. L. Kneebone, S. I. Gorelsky, I. Korobkov, S. Desgreniers, M. L. Neidig and S. Hill, *Dalton Trans.*, 2015, **44**, 10516 – 10523.

9 (a) T. J. Woods, H. D. Stout, B. S. Dolinar, K. R. Vignesh, M. F. Ballesteros-Rivas, C. Achim and K. R. Dunbar, *Inorg. Chem.*, 2017, **56**, 12094 – 12097; (b) M. A. Lemes, H. N. Stein, B. Gabidullin, K. Robeyns, R. Clérac and M. Murugesu, *Chem.-Eur. J.*, 2018, **24**, 4259 – 4263.

10 J.M. Rawson and J.J. Hayward, *"Reversible spin pairing in crystalline organic radicals"* in *Spin Crossover Materials: Properties and Applications* (M.A. Halcrow Ed), J. Wiley & Sons (2013).

11 (a) W. Fujita, K. Awaga, M. Takahashi, M. Takeda and T. Yamazaki, *Chem. Phys. Lett.*, 2002, **362**, 97–102; (b) W. Fujita and K. Awaga, *Chem. Phys. Lett.*, 2002, **357**, 385–388.

12 E.G. Awere, N. Burford, R.C. Haddon, S. Parsons, J. Passmore, J.V. Waszczak and P.S. White, *Inorg. Chem.*, 1990, **29**, 4821 – 4830.

13 W. Fujita, K. Awaga, Y. Nakazawa, K. Saito and M. Sorai, *Chem. Phys. Lett.*, 2002, **352**, 348 – 352.

14 (a) W.Fujita, K.Kikuchi, K.Awaga, *Angew. Chem. Int. Ed.*, 2008, **47**, 9480 – 9483; (b) W.Fujita, K.Awaga, R.Kondo, S.Kagoshima, *J. Amer. Chem. Soc.*, 2006, **128**, 6016 – 6017.

15 W. Fujita and K. Awaga, *J. Amer. Chem. Soc.*, 2001, **123**, 3601 – 3602.

16 C. M. Lieberman, A. S. Filatov, Z. Wei, A. Y. Rogachev, A. M. Abakumov and E. V. Dikarev, *Chem. Sci*., 2015, **6**, 2835 – 2842.

17 (a) G. Wolmershäuser, M. Schnauber and T. Wilhelm, *Chem. Commun.*, 1984, 573 – 574; (b) G.D. McManus, J.M. Rawson, N. Feeder, F. Palacio and P. Oliete, *J. Mater. Chem.*, 2000, **10**, 2001 – 2003.

18 (a) A. Alberola, R. D. Farley, S. M. Humphrey, G. D. McManus, D. M. Murphy and J. M. Rawson, *Dalton Trans.*, 2005, 3838 – 3845; (b) G. D. McManus, J. M. Rawson, N. Feeder, E. J. L. McInnes,J. J. Novoa, R. Burriel, F. Palacio and P. Oliete, *J. Mater. Chem.*, 2001, **11**, 1992.

19 I. A. Gass, S. Tewary, G. Rajaraman, M. Asadi, D. W. Lupton, B. Moubaraki, G. Chastanet, J.-F. Létard and K. S. Murray, *Inorg. Chem*. 2014, **53**, 5055 – 5066.

20 *Magnetochemistry*, R.L. Carlin, Springer-Verlag (1986).

21 N. F. Chilton, R. P. Anderson, L. D. Turner, A. Soncini and K. S. Murray, *J. Comput. Chem.*, 2013, **34**, 1164 – 1175.

22 E. M. Fatila, R. Clérac, M. Jennings and K. E. Preuss, *Chem. Commun.*, 2013, **49**, 9431 – 9433.

